Ceramics International 47 (2021) 1837–1843

Contents lists available at ScienceDirect

Ceramics International

journal homepage: www.elsevier.com/locate/ceramint

A comparative study of silicon nitride and SiAlON ceramics against *E. coli*

Seniz R. Kushan Akin *, Caterina Bartomeu Garcia, Thomas J. Webster

Department of Chemical Engineering, Northeastern University, Boston, MA, 02115, USA

ARTICLE INFO

Keywords:
Silicon nitride
Si_3N_4
SiAlON
Bioceramics
Antibacterial

ABSTRACT

In recent decades, due to some limitations from alumina (Al_2O_3) and zirconia (ZrO_2), silicon nitride (Si_3N_4) has been investigated as a novel bioceramic material, mainly in situations where a bone replacement is required. Si_3N_4 ceramics and its derivative form, SiAlON, possess advantages in orthopedics due to their mechanical properties and biologically acceptable chemistry, which accelerates bone repair. However, biological applications require additional properties, enabling stronger chemical bonding to the surrounding tissue for better fixation and the prevention of bacteria biofilm formation. Therefore, two commercial Si_3N_4 and SiAlON ceramics were investigated in this study and compared to each other according to their material properties (like wetting angles and surface chemistry) and their antibacterial behaviors using *E. coli*. Results provided evidence of a 15% reduction in *E. coli* colonization after just 24 h on Si_3N_4 compared to SiAlON which is impressive considering no antibiotics were used. Further, a mechanism of action is provided. In this manner, this study provides evidence that Si_3N_4 should be further studied for a wide range of antibacterial orthopedic, or other suitable biomaterial applications.

1. Introduction

Silicon nitrides provide an excellent combination of material properties and have been intensively studied and widely used in structural applications at both room and elevated temperatures [1–6]. Their high fracture toughness - as a fact of their microstructural development - makes them resistant to impact and high wear resistance owing to the covalent nature of their bonding, paving the way for the use of these materials in bio-applications. Another principal advantage of using Si_3N_4 as a biomaterial is based on its biologically accepted elements. N is a natural component in the human body and Si ion release has been shown to contribute to osteoblast (bone forming cells) formation and to inhibit osteoclast (bone resorbing cells) activity [7,8]. Moreover, studies carried out in recent decades on Si_3N_4 ceramics also revealed their good bioactivity and osseointegration [9–14]; non-cytotoxicity [15–18] and because they are partially radiolucent, a better performance in visualization techniques than some other biomaterials [19].

However, despite the many different potential applications of Si_3N_4 in the human body, only spinal spacers are commercially available in the market. For example, successful outcomes of the first clinical study after a 30-year follow-up for lumbar fusion was reported by an Australian group [20]. Subsequent studies have shown effective bone ingrowth into porous Si_3N_4 even without an added autograft [19,21]. Moreover, in a recent in vivo study it was also explained that the osseointegration of Si_3N_4 occurred since the Si and N elements stimulated progenitor cell differentiation and osteoblastic activity, which ultimately resulted in accelerated bone ingrowth [21]. Si_3N_4 may also be particularly suitable in the treatment of pyogenic infectious discitis (infection of the discs between the vertebra of the spine) owing to its good antibacterial behavior [22], which was also reported by several other in vitro studies [10,11,23–25].

There have also been some in vitro studies of SiAlON ceramics indicating their viability for clinical applications [26–28]. SiAlONs are solid solutions of Si_3N_4 with Al_2O_3, in which silicon and nitrogen are replaced by aluminum and oxygen, respectively. The two forms of SiAlON ceramics are α-SiAlON (abbreviated as α′) and β-SiAlON (β′) and they have advantages of better sinterability, wide compositional design between full α′ and full β’ compositions, and different intergranular phase chemistry over Si_3N_4 ceramics, which effects their mechanical properties [29]. Densification of both Si_3N_4 and SiAlON requires the addition of metal oxides in order to form liquid phases at evaluated temperatures and provides liquid phase sintering which, when cooled, remains as an intergranular oxynitride glassy phase. This intergranular film is approximately 1–1.5 nm thick and plays a key role in identifying the mechanical and high temperature properties of Si_3N_4 and related materials [30–33]. Therefore, in reality, Si_3N_4 and SiAlON ceramics are

* Corresponding author. Cankaya University, Department of Materials Science and Engineering, 06790, Ankara, Turkey.
E-mail address: senizakin@cankaya.edu.tr (S.R. Kushan Akin).

https://doi.org/10.1016/j.ceramint.2020.09.012
Received 25 June 2020; Received in revised form 18 August 2020; Accepted 1 September 2020
Available online 11 September 2020

like composite systems where grains are distributed in a glassy grain boundary phase. Moreover, the glassy grain boundary phase may exhibit different biochemical properties from the Si_3N_4 crystal itself and there are also several studies supporting this behavior [13,17,34]. When two ceramic materials have been compared, SiAlONs offer the advantages of incorporating some of the sintering additives into the lattice structure, thus, reducing the overall amounts of a grain boundary phase and potentially improving properties especially at elevated temperatures compared to Si_3N_4 [29]. This is also believed to be effective towards their antibacterial behavior when compared to Si_3N_4, which is investigated in this paper.

Therefore, in this study, two commercial Si_3N_4 and SiAlON ceramics were investigated together and compared to understand the effect of the change in chemistry and structure on bio properties like bacterial resistance.

2. Experimental procedures

2.1. Materials

The materials used in this study, Si_3N_4 and SiAlON, were supplied by a commercial company (MDA Advanced Ceramics Ltd.). They were both sintered via gas pressure sintering with densification additives, similar to the methods previously reported [35,36]. Some manufacturing details of these ceramic are as follows: the Si_3N_4 powder (Ube SN E−10, Ube City, Japan) was first mixed with sintering aids (Al_2O_3, Er_2O_3, Sm_2O_3 and CaO for the SiAlON and Y_2O_3-HfO_2-MgO for the Si_3N_4) and cold-pressed at room temperature into square-shaped samples. For the production of Si_3N_4, sintering additives other than Al_2O_3 were used and for the SiAlON system, Al_2O_3 was also introduced into the system as well as other sintering aids. Then, the cold-pressed samples were sintered under nitrogen via gas pressure sintering at a temperature in excess of 1700 °C. Both materials were used in the as-received (as-fired) condition. Ultrasonic surface cleaning was performed by acetone, ethanol and deionized water (15 min each) before evaluation.

2.2. Characterization

2.2.1. Density measurements

Bulk density was measured by the Archimedes method using deionized water as an immersion medium. Theoretic density measurements were calculated according to the bulk density results known from the literature data.

2.2.2. Microstructural analysis

Microstructures of the as-fired surfaces of the bulk samples were observed using a scanning electron microscope (SEM) (Hitachi S-4800) equipped with a field emission gun using a secondary electron imaging mode. Samples were Pt coated before observation.

2.2.3. Phase characterization/molecular spectroscopy analyses

Phase identification of the samples was performed by X-ray diffraction analysis (XRD) (RINT2200, Rigaku, Tokyo, Japan) with CuKα ($\lambda = 1.54056$ Å) radiation at a scan speed of 1°/min between 20 and 60 2θ angles. Quantitative analysis of the α′ and β′ phases was carried out according to the integrated intensities of the (102) and (210) reflections of α′ and the (101) and (210) reflections of β' by the following equation [37]:

$$I\beta/I\beta + I\alpha = 1/1 + \mathrm{K}[(1/w\beta) - 1] \quad (1)$$

where Iα and Iβ are the observed intensities of the α′ and β′ peaks, respectively, wβ is the relative weight fraction of β′, and K is the combined proportionality constant resulting from the constants in the two equations:

$$I\beta = K\beta * W\beta \quad (2)$$

$$I\alpha = K\alpha * W\alpha \quad (3)$$

K was taken as 0.518 for β (101) – α (102) reflections and 0.544 for β (210) – α (210) reflections [38].

X-ray photoelectron spectroscopy (XPS) was performed using a spectrometer (SPECS Phoibos 100 spectrometer) employing an Al-Kα monochromatic X-ray source. Low-resolution spectral scans were conducted using a pass energy of 200 eV. Data processing was performed with CasaXPS software (Casa software Ltd, Cheshire, UK).

2.2.4. Contact angle measurements

In order to assess the wetting characteristics of the samples, a drop shape analysis system (Phoenix 150 Contact Angle Analyzer) was used. The system consisted of an optical tensiometer equipped with a CCD video camera having a specially designed optical system for reducing light scattering and mounting an easy camera with 'all direction' adjustment. Drops were deposited on the surfaces, at room temperature, through a needle. Along the test substrates, contact angle measurements were performed in triplicate. Images were snapped 5 s after the solvent droplets were deposited onto the surfaces under ambient temperature conditions. Longer times were avoided because of either the importance of the early surface interaction between the biological fluids and the solid surface or to prevent changes of the contact angle deriving from secondary effects like solid/liquid reactions or liquid evaporation [39].

2.3. Bacteria studies

Samples were tested against a Gram-negative bacteria, *Escherichia coli (E. coli*, ATCC 25922), by a broth dilution test to study. Bacteria were obtained from the American Type Culture Collection (Manassas, VA). Separate Tryptic Soy Broth (TSB) media were inoculated with one colony of bacteria and the bacteria were cultured on a shaking flask at 37 °C for 24 h. Samples were put in a well plate and covered with the prepared bacteria solution at an initial concentration of 10^5 cells/mL, which was prepared using optical absorbance. Each system was tested using three samples. After incubation for 24 h, samples were washed with a phosphate buffer solution (PBS) and introduced in the proper tubes with a proper amount of PBS added and sonicated for 10 min followed by vortexing for 10 s before preparing four different dilutions (1:1000, 1:10000, 1:100000, and 1:1000000) of each sample. Three 10 μl droplets of each dilution were dropped onto the petri dishes overlaid by solidified mixtures containing 1.5% of agar and 3.0% of TSB and were allowed to air dry for 15 min in a sterile environment. The plates were then incubated in a stationary incubator operating at 5% CO_2 and 37 °C for 12 h until the colonies formed and reached a size that could be counted. Since the sizes of the samples were not equal to each other, area calculations were carried out and normalized by the bacteria results. When calculating the area of the samples, a surface that was in contact with the base of the well plate was subtracted since the bacteria were not able to attach to that bottom surface.

2.4. Statistical analysis

All of the reported values represent the average of three independent experiments. Standard errors of the mean were calculated in order to define data uncertainty, and representative error bars were included for all data figures. Analysis of the results was carried out using the student's t-test, with a significance level of $p < 0.25$.

3. Results and discussion

3.1. Characterization results

3.1.1. Density, phase characterization (XRD), molecular spectroscopy analyses (XPS) and contact angle measurements

Density measurements of the bulk samples revealed 100% theoretical density (TD) as seen in Table 1.

Phase characterization results of the Si_3N_4 and SiAlON samples are given in Fig. 1. XRD patterns showed that the main crystalline phase was β- Si_3N_4 with traces of α- Si_3N_4. A slight shifting of the peaks in the SiAlON sample was observed when compared with Si_3N_4 as a result of a change in the lattice structure of Si_3N_4 by the incorporation of Al and O atoms. Although α-SiAlON is based on α- Si_3N_4 and β-SiAlON is based on β-Si_3N_4 hexagonal structures, the change in the XRD patterns caused by the change in lattice parameters was obvious. α-SiAlON and β-SiAlON are designated in Fig. 2 as α′ and β′, respectively. As a result of this quantitative calculation, the α': β' ratio was found as 50:50 for the SiAlON sample (Table 1).

The XPS data given in Fig. 2 indicate the changes in surface chemistry due to the different nitride/oxide atomic ratios. Surface characterization carried out by XPS also revealed the high amount of the oxynitride grain boundary phase in the Si_3N_4 samples (Fig. 2). According to these results, the O/Si atomic ratios of Si_3N_4 and SiAlON samples were 2.00 and 0.59, respectively, which appeared to be a surface grain boundary oxide phase rich in Si_3N_4.

Wetting angles measured at the fifth second after placing the water drop revealed a significant change in wettability between both materials (Fig. 3). A dramatic change was observed in contact angles in the samples as 76° and 101° for Si_3N_4 and SiAlON samples, respectively. These results demonstrated a more hydrophilic character of Si_3N_4 compared to SiAlON.

3.1.2. Microstructural analysis results

Secondary electron images of the as-fired surfaces of the Si_3N_4 and SiAlON samples revealed similar microstructural development of the samples with some large elongated grains dispersed in finer elongated microstructures, which is typical for β-Si_3N_4 and β-SiAlON grains (Fig. 4).

3.2. Bacteria and cell culture results

The results from the antibacterial tests of both samples against *E. coli* via colony counting assays are given in Fig. 5.

Results showed a statistical difference (at $p < 0.25$) between the number of colonies between the SiAlON and Si_3N_4 materials with Si_3N_4 possessing better (15%) antibacterial properties against *E. coli* after 24 h. Due to the microstructural similarity between the samples given in Fig. 4, close antibacterial results was not surprising. However, it is a well-known fact that bacterial response to a material not only depends on roughness (which is a fact of microstructure) but also on the chemical composition which collectively contribute to surface energy.

4. Discussion

As a result of liquid phase sintering, Si_3N_4 based ceramics form a composite like structure in its final form consisting of polycrystalline Si_3N_4 grains distributed in an oxynitride intergranular glass (if additional heat treatment is applied, this phase can be turned into crystalline phase). In the case of Si_3N_4, sintering additives that aids densification always exists in the grain boundary phase, whereas aluminum Al and O partially replaces with Si and N in the SiAlON system. Moreover, additional sintering additives rather than Al_2O_3, which are Er-Sm-Ca in the SiAlON sample investigated in this study, can also incorporate into the α-SiAlON to stabilize this structure by filling the interstitial sites. This makes a reduction in the grain boundary phase amount in the final material and the grain/oxygen rich grain boundary phase ratio variation makes differences in the surface properties of Si_3N_4 and SiAlON ceramics. Comparison of N/Si and O/Si ratios of the samples measured by XPS analysis indicate the lower amount of O/Si and higher N/Si ratio in SiAlON sample as a result of reduction in oxygen rich grain boundary phase. According to the XRD results, the SiAlON sample consisted of 50% α-SiAlON with a decreased grain boundary phase amount because of the reason explained above. The surface reactivity of Si_3N_4 induced the formation of a thin layer composed of mainly silanol (Si–OH) and secondary amine groups (Si2–NH) [40]. Therefore XPS results also point out that the amine/silanol groups ratio is higher in SiAlON sample.

Effect of O/Si and N/Si ratios on the surface properties were also investigated before for Si_3N_4 samples after thermal, chemical, and mechanical treatments in order to induce changes in surface composition [41]. The results showed that specimens with higher N/Si and lower O/Si ratios were achieved after such treatments (than the as-fabricated one) exhibited strong negative surface charging at homeostatic pH and moderate hydrophilicity was observed.

The relatively high contact angle on SiAlON in this study compared to Si_3N_4 as clearly seen in Fig. 3, can be explained on the basis of the interaction energy at the solid/liquid interface which can also be attributed to the reduced amount of grain boundary phases. Previous studies have also indicated that increasing the grain boundary phase amount caused a decrease in the wetting angle making the surface more hydrophilic [42]. The quantitative indicator of hydrophilicity is given by polarity. In the abundance of oxygen rich phase there is a better affinity towards water since the polar forces also act at the interfere, in addition to dispersion ones, and hyrophilicity increases. For the Si_3N_4 sample, it was observed that the volume of the oxygen was larger and thus, it was observed to be more hydrophilic compared to SiAlON.

Bacteria such as *E. coli* cause harmful effects to humans and is still known to be the basic problem for implants. Some materials show the ability to kill bacteria by the release of diverse antibacterial species, like reactive oxygen species (ROS) and the metallic ions. The bacterial adherence to Si_3N_4 is believed to be a result of multivariate mechanisms [23,24,43] The reported mechanisms in previous studies both depend on the surface morphology and the chemistry.

Nanostructured surface morphology have been reported to exhibit antimicrobial properties [44–46]. It has been suggested that the damage to cell membranes by these nano-rough structures might occur through changes to the expression of genes related to the cell membrane [44]. The surface nanostructure influences their ability to affect the activity of bacteria [47,48]. Their antimicrobial mechanisms are presumably related to disorder or denaturation of cell walls. However, there are no investigations from the biophysical viewpoint about the interactions between nanostructured surfaces and the cell wall, and the origin of the antimicrobial activity of nanostructured surfaces is unknown.

Due to the microstructural similarity between the samples given in Fig. 4, close antibacterial results was not surprising. However, bacterial response to a material not only depends on roughness (which is a fact of microstructure for the samples used as fired) but also on the chemical composition as explained above which collectively contribute to surface energy and the surface charge which is quite important for the antibacterial behavior. Since most bacteria exhibit a negative surface charge at a physiological pH value [49,50], the electrostatic component of the bacteria-surface interaction will be repulsive if the surface of the material also exhibits a negative charge. Moreover, the magnitude of the repulsion will increase as the magnitude of the surface charge increases. The surface charge of the material in biological media, where the pH is

Table 1
Percent theoretical density and phase ratio of the samples.

Sample	%TD	Phase Composition
Si3N4	~100	~100% β-Si_3N_4
SiAlON	~100	50% β-SiAlON + 50% α-SiAlON

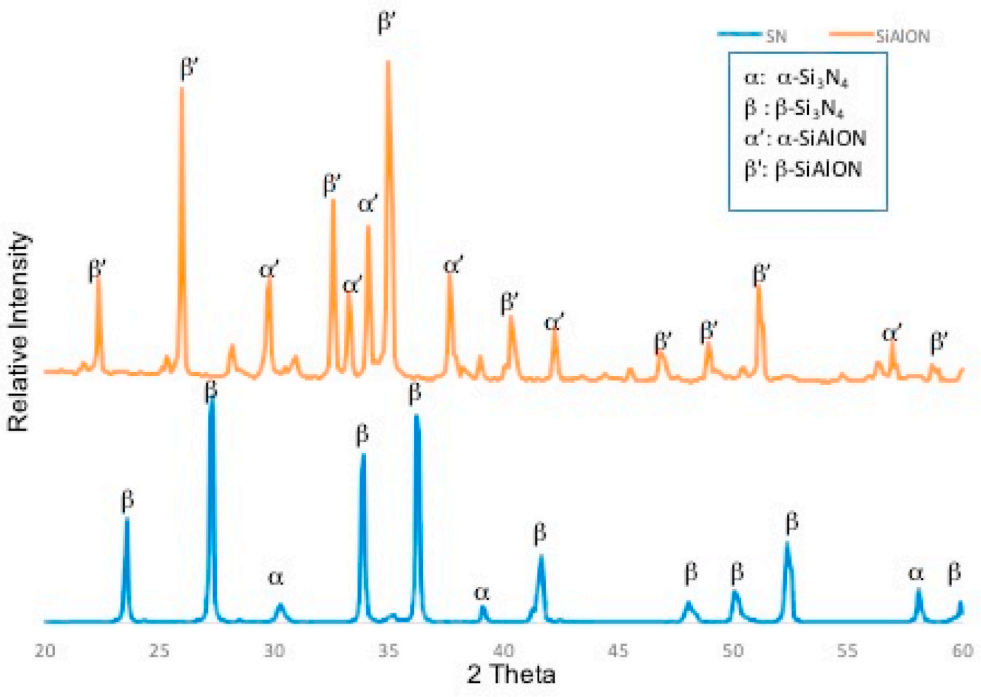

Fig. 1. XRD results of the samples.

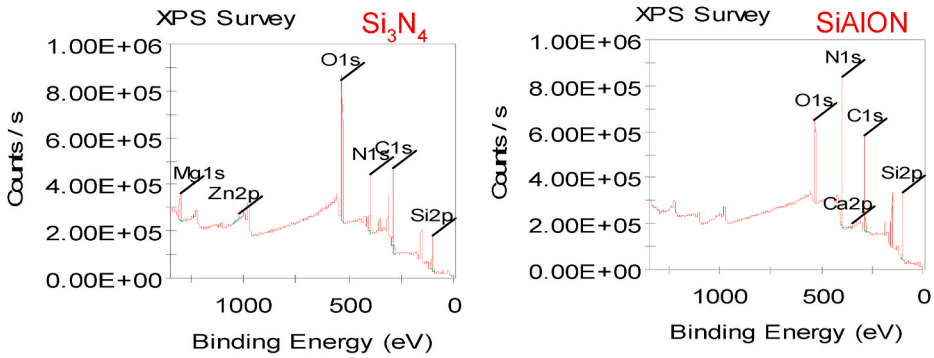

Sample	Si (at.%)	N (at.%)	O (at.%)		N/Si	O/Si
Si_3N_4	13.26	16.46	26.62		1.24	2.00
SiAlON	21.96	31.30	12.99		1.43	0.59

Fig. 2. XPS results of the samples.

around 7.4, is estimated by the isoelectric point (IEP). It is well known that if the pH of the media is greater than the IEP, than the surface of the material will be negatively charged. Therefore, the lower the IEP of the surface, the better the repulsion of the bacteria will be. For the pure Si_3N_4 IEP is known to be around ~9.3–9.7 [41,51] which causes a positive surface charge, whereas SiO2 has a value of ~2–3 [41,52] and, therefore, results in a negative surface charge. As previously explained, Si_3N_4 or SiAlON grains are distributed within a continuous grain boundary phase, which should have an IEP lower than the grains since grain boundary phase is rich in oxygen content. In this study, since the Si_3N_4 sample is expected to have a lower IEP (as a result of having a higher O/Si and lower N/Si ratio on the surface, as determined by XPS in Fig. 2), the prevention of bacteria colonization was slightly more successful. Therefore, the difference in surface chemistry given in Fig. 2 which also confirms the wetting behavior given in Fig. 3, are reasons for the slight improvement in the antibacterial behavior of Si_3N_4 ceramics. It is known from the previous studies that the antibacterial properties could be improved by increasing the number of amine rich surfaces, as they can repel bacteria [41]. This is believed to be happened in the SiAlON system. These amine groups release ammonia (NH3) and silicic acid (H4SiO4) into biological fluids and NH3 is converted into peroxynitride anion (O═NOO) which is toxic to bacteria.

As it was discussed before by Bock et al. [24], favorable antibacterial mechanisms of Si_3N_4 were depend on multi tasks and can be improved by fine surface topography, negative charging for repulsion, chemical interactions like peroxynitride anion formation and hydrophilicity. Furthermore, as a result of similar microstructure, there was a balance between the advantages of silanol and amine groups towards reducing

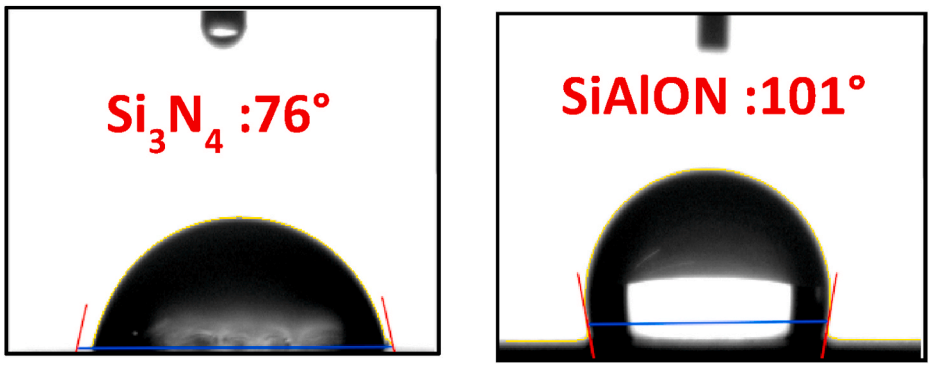

Fig. 3. Contact angles of the samples.

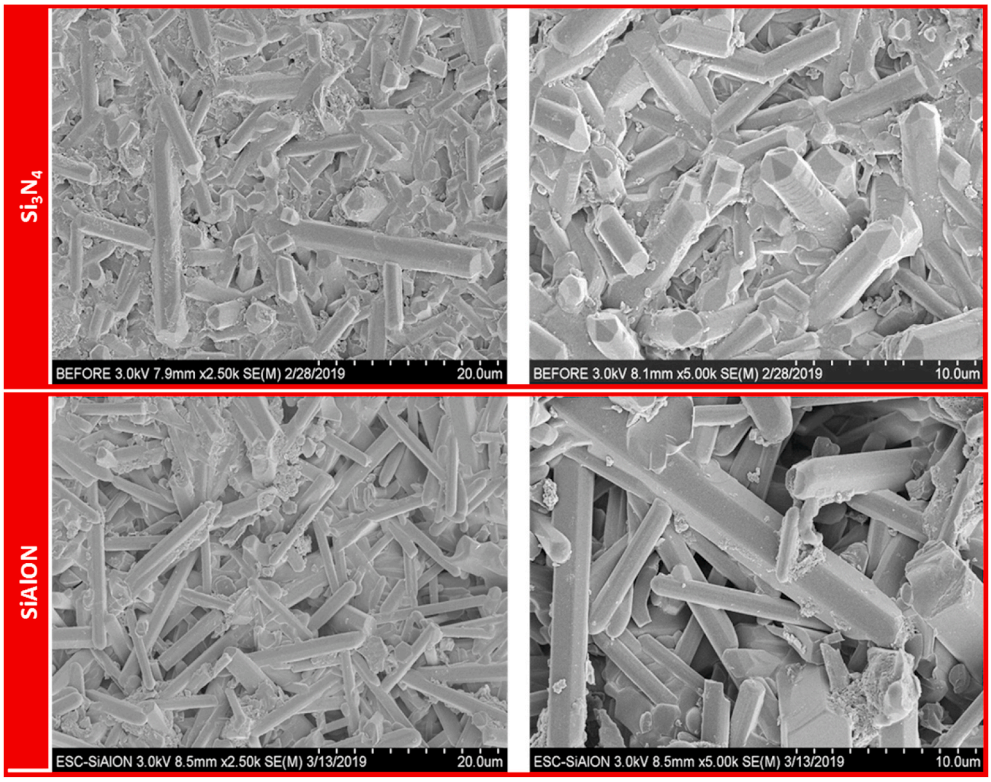

Fig. 4. SE images of Si_3N_4 and SiAlON samples at different magnifications.

bacteria on Si_3N_4 and SiAlON, respectively.

5. Conclusion

The biophysical properties expected from Si_3N_4 and related materials include its high surface energy (low wetting angle and high hydrophilicity) and negative surface charge for better osteointegration and to repel bacteria. In this study, *E. coli* colonization on two commercial Si_3N_4 and SiAlON (50%α': 50%β') ceramics with similar microstructures were examined. Results showed:

- A high amount of silanol groups were observed due to the higher amount of O/Si in Si_3N_4 ceramics. This behavior is believed to be related with a decrease in the amount of grain boundary phases for the SiAlON ceramics.
- In the Si_3N_4 and related systems, hydrophilic surfaces are preferred since in general less bacterial attachment has been observed on such surfaces. In this study system, Si_3N_4, the system with the higher grain boundary phase amount showed a more hydrophilic character.
- The antibacterial behavior against *E. coli* was similar between the two systems but an improvement was observed for Si_3N_4 due to the combination of the hydrophilicity of Si_3N_4 and a reduction of grain boundary phase amount as well as the amine rich surface of SiAlON, which slightly increased bacteria colonization.
- For various applications, SiAlON ceramics are known to be advantageous over Si_3N_4 by means of better sinterability and possibility of control of mechanical properties by the control in α'/β' composition design. The results of this study showed that SiAlON ceramics show promise even in orthopedic applications as a result of antibacterial behavior similar to Si_3N_4.

Declaration of competing interest

The authors declare that they have no known competing financial interests or personal relationships that could have appeared to influence

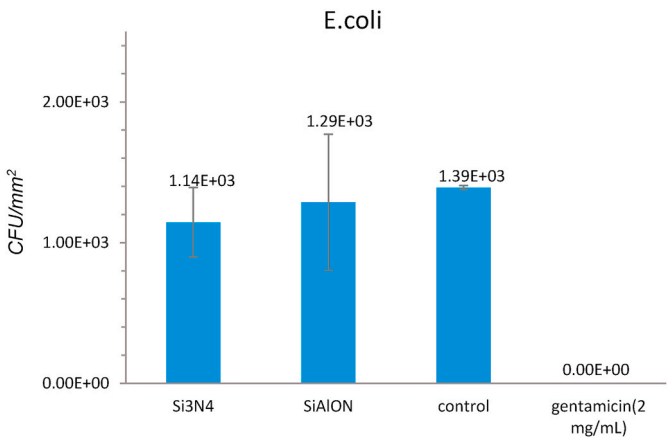

Fig. 5. Comparison of bacterial growth on Si_3N_4 and SiAlON (Data = ±SD; n = 3). *E. coli* colonization of Si_3N_4 was statistically less than SiAlON at $p < 0.25$.

the work reported in this paper.

Acknowledgements

One of the authors, Seniz R. Kushan Akin, would like to thank The Scientific and Technological Research Council of Turkey (TUBITAK) for funding her studies at Northeastern University through the 2219 Fellowship Programme.

References

[1] F.L. Riley, Silicon nitride and related materials, J. Am. Ceram. Soc. 83 (2000) 245–265.
[2] G. Petzow, M. Herrmann, Silicon nitride ceramics, Struct. Bond 102 (2002) 47–167.
[3] G. Ziegler, J. Heinrich, G. Wötting, Review-relationships between processing, microstructure and properties of dense and reaction-bonded silicon nitride, J. Mater. Sci. 22 (1987) 3041–3086.
[4] J.F. Yang, T. Ohji, K. Niihara, Influence of yttria alumina content on sintering behavior and microstructure of silicon nitride ceramics, J. Am. Ceram. Soc. 83 (8) (2000) 2094–2096.
[5] N. Hirosaki, A. Okada, K. Matoba, Sintering of Si3N4 with the addition of rare-earth oxides, J. Am. Ceram. Soc. 71 (3) (1988) 144–147.
[6] M.H. Bocanegra-Bernal, B. Matovic, Mechanical properties of silicon nitride-based ceramics and its use in structural applications at high temperatures, Mater. Sci. Eng. A527 (2010) 1314–1338.
[7] Z. Mladenovic, A. Johansson, B. Willman, K. Shahabi, E. Bjorn, M. Ransjo, Soluble silica inhibits osteoclast formation and bone resorption in vitro, Acta Biomater. 10 (1) (2014) 406–418.
[8] G. Pezzotti, R.M. Bock, T. Adachi, A. Rondinella, F. Boschetto, W. Zhu, E. Marin, B. J. McEntire, B.J. McEntire, B.S. Bal, O. Mazda, Silicon nitride surface chemistry: a potent regulator of mesenchymal cell activity for bone formation, Appl. Mater. Today 9 (2017) 82–95.
[9] G. Pezzotti, N. Oba, W. Zhu, E. Marin, A. Rondinella, F. Boschetto, B. McEntire, K. Yamamoto, B.S. Bal, Human osteoblasts grow transitional Si/N apatite in quickly osteointegrated Si_3N_4 cervical insert, Acta Biomater. 64 (2017) 411–420.
[10] D.J. Gorth, S. Puckett, B. Ercan, T.J. Webster, M. Rahaman, B.S. Bal, Decreased bacteria activity on Si_3N_4 surfaces compared with PEEK or titanium, Int. J. Nanomed. 7 (2012) 4829–4840.
[11] T.J. Webster, A.A. Patel, M.N. Rahaman, B.S. Bal, Anti-Infective and osteointegration properties of silicon nitride, poly (Ether ether ketone), and titanium implants, Acta Biomater. 8 (2012) 4447–4454.
[12] E. Marin, S. Horiguchi, M. Zanocco, F. Boschetto, A. Rondinella, W. Zhu, R. M. Bock, B.J. McEntire, T. Adachi, B.S. Bal, G. Pezzotti, Bioglass functionalization of laser-patterned bioceramic surfaces and their enhanced bioactivity, Heliyon 4 (2018), e01016.
[13] C.C. Guedes-Silva, A.C. Dorion Rodas, A.C. Silva, C. Ribeiro, F.M. de Souza Carvalho, O.Z. Higa, T.S. Ferreira, Microstructure, mechanical properties and in vitro biological behavior of silicon nitride ceramics, Mater. Res. 21 (6) (2018), e20180266.
[14] S. Lal, E.A. Caseley, R.M. Hall, J.L. Tipper, Biological impact of silicon nitride for orthopaedic applications: role of particle size, Surface Composition and Donor Variation, Scientific REPORTS 8 (2018) 9109.
[15] C.C. Guedes-Silva, O.Z. Higa, J.C. Bressiani, Cytotoxic evaluation of silicon nitride-based ceramics, Mater. Sci. Eng. C 24 (5) (2004) 643–646.
[16] C. Santos, S. Ribeiro, J.K.M.F. Daguano, S.O. Rogero, K. Strecker, C.R.M. Silva, Development and cytotoxicity evaluation of SiAlONs ceramics, Mater. Sci. Eng. C 27 (1) (2007) 148–153.
[17] M. Mazzocchi, A. Bellosi, On the possibility of silicon nitride as a ceramic for structural orthopaedic implants. Part I: processing, microstructure, mechanical properties, cytotoxicity, J. Mater. Sci. Mater. Med. 19 (2008) 2881–2887.
[18] M. Precnerova, K. Bodisova, F. Frajkorova, D. Galuskova, Z.V. Novakova, J. Vojtassak, Z. Lences, P. Sajgalik, In vitro bioactivity of silicon nitride-hydroxyapatite composites, Ceram. Int. 41 (6) (2015) 8100–8108.
[19] M.P. Arts, J.F.C. Wolfs, T.P. Corbin, Porous silicon nitride spacers versus PEEK cages for anterior cervical discectomy and fusion: clinical and radiological results of a single-blinded randomized controlled trial, Eur. Spine J. (2017) 1–8.
[20] R.J. Mobbs, P.J. Rao, K. Phan, P. Hardcastle, W. Jie Choy, E.R. McCartney, R. K. Druitt, C.A.L. Mouatt, C.C. Sorrell, Anterior lumbar interbody fusion using reaction bonded silicon nitride implants: long-term case series of the first synthetic anterior lumbar interbody fusion spacer implanted in humans, World Neurosurg 120 (2018) 256–264.
[21] M.C. Anderson, R. Olsen, Bone ingrowth into porous silicon nitride, J. Biomed. Mater. Res. 92A (2010) 1598–1605.
[22] W.M. Rambo Jr., Treatment of lumbar discitis using silicon nitride spinal spacers: a case series and literature review, International Journal of Surgery Case Reports 43 (2018) 61–68.
[23] G. Pezzotti, R.M. Bock, B.J. McEntire, E. Jones, M. Boffelli, W. Zhu, G. Baggio, F. Boschetto, L. Puppulin, T. Adachi, T. Yamamoto, N. Kanamura, Y. Marunaka, B. S. Bal, Silicon nitride bioceramics induce chemically driven Lysis in Porphyromonas Gingivalis, Langmuir 32 (2016) 3024–3035.
[24] R.M. Bock, E.N. Jones, D.A. Ray, B.S. Bal, G. Pezzotti, B.J. McEntire, Bacteriostatic behavior of surface-modulated silicon nitride in comparison to polyethereetherketone and titanium, J. Biomed. Mater. Res. 105 (2017).
[25] F. Boschetto, T. Adachi, S. Horiguchi, D. Fainozzi, F. Parmigiani, E. Marin, W. Zhu, B.J. McEntire, T. Yamamoto, N. Kanamura, O. Mazda, E. Ohgitani, G. Pezzotti, Monitoring metabolic reactions in Staphylococcus epidermidis exposed to silicon nitride using in situ time-lapse Raman spectroscopy, J. Biomed. Optic. 23 (5) (2018), 056002.
[26] C. Santos, S. Ribeiro, J.K.M.F. Daguano, S.O. Rogero, K. Strecker, C.R.M. Silva, Development and cytotoxicity evaluation of SiAlONs ceramics, Mater. Sci. Eng. C 27 (2007) 148–153.
[27] A. Kumar, A. Kumar Mallik, N. Calis Acikbas, M. Yaygıngol, F. Kara, H. Mandal, D. Basu, K. Biswas, B. Basu, Cytocompatibility property evaluation of gas pressure sintered SiAlON–SiC composites with L929 fibroblast cells and Saos-2 osteoblast-like cell, Mater. Sci. Eng. C 32 (2012) 464–469.
[28] A. Kumar Mallik, N. Calis Acikbas, F. Kara, H. Mandal, D. Basu, A comparative study of SiAlON ceramics, Ceram. Int. 38 (2012) 5757–5767.
[29] A. Rosenflanz, Silicon nitride and sialon ceramics, Curr. Opin. Solid State Mater. Sci. 4 (1999) 453–459.
[30] P.F. Becher, E.Y. Sun, K.P. Plucknett, K.B. Alexander, C.H. Hsueh, H.T. Lin, S. B. Waters, C.G. Westmoreland, E.S. Kang, K. Hirao, M.E. Brito, Microstructural design of silicon nitride with improved toughness: I, effects of grain shape and size, J. Am. Ceram. Soc. 81 (11) (1998) 2821–2830.
[31] P.F. Becher, G.S. Painter, E.Y. Sun, C.H. Hsue, M.J. Lance, The importance of amorphous intergranular films in self-reinforced Si_3N_4 ceramics, Acta Mater. 48 (18–19) (2000) 4493–4499.
[32] J. Yang, J.F. Yang, S.Y. Shan, J.Q. Gao, T. Ohji, Effect of sintering additives on microstructure and mechanical properties of porous silicon nitride ceramics, J. Am. Ceram. Soc. 89 (12) (2006) 3843–3845.
[33] W. Han, Y. Li, G. Chen, Q. Yang, Effect of sintering additive composition on microstructure and mechanical properties of silicon nitride, Mater. Sci. Eng. 700 (2017) 19–24.
[34] M. Amaral, M.A. Lopes, J.D. Santos, R.F. Silva, Wettability and surface charge of Si_3N_4–bioglass composites in contact with simulated physiological liquids, Biomaterials 23 (20) (2002) 4123–4129.
[35] H. Mandal, F. Kara, A. Kara, S. Turan, inventors, Doped Alpha-Beta Sialon Ceramics, United States patent US7064095B2, 2002.
[36] N. Calis Acikbas, H. Yurdakul, H. Mandal, F. Kara, S. Turan, A. Kara, B. Bitterlich, Effect of sintering conditions and heat treatment on the properties, microstructure and machining performance of α-β-SiAlON ceramics, J. Eur. Ceram. Soc. 32 (7) (2012) 1321–1327.
[37] R.G. Pigeon, A. Varma, Quantitative phase Analysis of Si_3N_4 by X-ray diffraction, J. Mater. Sci. Lett. 11 (1992) 1370–1372.
[38] K. Liddell, X-Ray Analysis of Nitrogen Ceramic Phases, MSc. Thesis, University of Newcastle, Upon Tyne, UK, 1979.
[39] M. Mazzocchi, D. Gardini, P.L. Traverso, M.G. Faga, A. Bellosi, On the possibility of silicon nitride as a ceramic for structural orthopaedic implants. Part II: chemical stability and wear resistance in body environment, J. Mater. Sci. Mater. Med. 19 (2008) 2889–2901.
[40] A. Bondanini, F. Monteverde, A. Bellosi, Influence of powder characteristics and powder processing routes on microstructure and properties of hot pressed silicon nitride materials, J. Mater. Sci. 36 (2001) 4851–4862.
[41] R.M. Bock, B.J. McEntire, B.S. Bal, M.N. Rahaman, M. Boffelli, G. Pezzotti, Surface modulation of silicon nitride ceramics for orthopaedic applications, Acta Biomater. 26 (2015) 318–330.
[42] M. Mazzocchi, D. Gardini, P.L. Traverso, M.G. Faga, A. Bellosi, On the possibility of silicon nitride as a ceramic for structural orthopaedic implants. Part II: chemical stability and wear resistance in body environment, J. Mater. Sci. Mater. Med. 19 (2008) 2889–2901.

[43] M. Ishikawa, K.L.D.M. Bentley, B.J. McEntire, B.S. Bal, E.M. Schwarz, C. Xie, E. Avenue, Surface topography of silicon nitride affects antimicrobial and osseointegrative properties of tibial implants in a murine model, J. Biomed. Mater. Res. 105 (2017) 3413–3421, https://doi.org/10.1002/jbm.a.36189.
[44] L. Rizzello, et al., Impact of nanoscale topography on genomics and proteomics of adherent bacteria, ACS Nano 5 (2011) 1865–1876.
[45] E.P. Ivanoa, et al., Natural bactericidal surfaces: mechanical rupture of pseudomonas aeruginosa cells by Cicada wings, Small 16 (2012) 2489–2494.
[46] E.P. Ivanoa, et al., Bactericidal activity of black silicon, Nat. Commun. 4 (2013) 2838–2844.
[47] K. Anselme, et al., The interaction of cells and bacteria with surfaces at the nanometer scale, Aca Biomaterialia 6 (2010) 3824–3846.
[48] Li-Chong Xu, Christopher A. Siedlecki, Submicron-textured biomaterial surface reduces staphylococcal bacterial adhesion and biofilm formation, Acta Biomater. 8 (1) (2012) 72–81.
[49] V.P. Hairden, J. Harris, The isoelectric point of bacterial cells, J. Bacteriol. 65 (1953) 198–202.
[50] M. Horka, P. Karasek, F. Ruzicka, M. Dvorackova, M. Sittova, M. Roth, Separation of methicillin-resistant from methicillin-susceptible Staphylococcus aureus by electrophoretic methods in fused silica capillaries etched with supercritical water, Anal. Chem. 86 (2014) 9701–9708.
[51] P. Greil, R. Nitzsche, H. Friedrich, W. Hermel, Evaluation of oxygen content on silicon nitride powder surface from the measurement of the isoelectric point, J. Eur. Ceram. Soc. 7 (1991) 353–359.
[52] J.A. Lewis, Colloidal processing of ceramics, J. Am. Ceram. Soc. 83 (2000) 2341–2359.